REPORT DOCUMENTATION PAGE

AFRL-SR-BL-TR-98-
0457

Public reporting burden for this collection of information is estimated to average 1 hour per response, including the time for reviewing instructions, ~~~~~~~ ~~~rces, gathering and maintaining the data needed, and completing and reviewing the collection of information. Send comments regarding this burden estimate or any other aspect of this collection of information, including suggestions for reducing this burden, to Washington Headquarters Services, Directorate for Information Operations and Reports, 1215 Jefferson Davis Highway, Suite 1204, Arlington, VA 22202-4302, and to the Office of Management and Budget, Paperwork Reduction Project (0704-0188), Washington, DC 20503.

1. AGENCY USE ONLY *(Leave blank)*	2. REPORT DATE May 12, 1998	3. REPORT TYPE AND DATES COVERED Final Report (08/15/97 – 02/14/98)	
4. TITLE AND SUBTITLE "Ionic Self-Assembled Monolayer (ISAM) Nonlinear Optical Thin Films and Devices"		**5. FUNDING NUMBERS** F49620-97-C-0047 STTR/TS 65502F	
6. AUTHORS Michael B. Miller			
7. PERFORMING ORGANIZATION NAME(S) AND ADDRESS(ES) F&S, Inc. 2801 Commerce Street P.O. Box 11704 Blacksburg, VA 24060 Blacksburg, VA 24062-1704		**8. PERFORMING ORGANIZATION REPORT NUMBER** AFR-1T-3010	
9. SPONSORING/MONITORING AGENCY NAME(S) AND ADDRESS(ES) AFOSR 110 Duncan Ave., Room B115 Bolling AFB, DC 20332-8050		**10. SPONSORING/MONITORING AGENCY REPORT NUMBER**	

11. SUPPLEMENTARY NOTES

19980602 033

12a. DISTRIBUTION/AVAILABILITY STATEMENT

Approved for public release;
distribution unlimited.

13. ABSTRACT *(Maximum 200 words)*

During the performance of this STTR Phase I program, F&S along with our development partners at Virginia Tech, have successfully demonstrated the formation of noncentro-symmetric thin films using the ISAM process. These films exhibit significant second-order nonlinear optical properties. Further, we have demonstrated a fabrication process capable of creating thousands of bilayers of such films, which demonstrates the feasibility of full-scale commercial manufacturing. The resulting films exhibit significant robustness, particularly during temperature cycling, and do not have to be poled to achieve their nonlinear properties. Finally, we have shown increased performance of the ISAM films through the synthesis of a number of new polydye materials. These Phase I program results lay the foundation for an expanded product development program based on this technology.

14. SUBJECT TERMS nonlinear optics, thin-film waveguides, noncentrosymmetric ordering, frequency conversion, ionic self-assembled monolayer (ISAM)			15. NUMBER OF PAGES 31
			16. PRICE CODE
17. SECURITY CLASSIFICATION OF REPORT Unclassified	18. SECURITY CLASSIFICATION OF THIS PAGE Unclassified	19. SECURITY CLASSIFICATION OF ABSTRACT Unclassified	20. LIMITATION OF ABSTRACT

Ionic Self-Assembled Monolayer (ISAM) Nonlinear Optical Thin Films and Devices

Final Technical Report

Performance Period: 15 August 1997 - 14 February 1998

AFOSR STTR Contract No.   F49620-97-C-0047

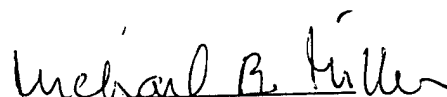Technical Monitor: Charles Y-C Lee
                            Directorate of Chemistry and Life Sciences
                            110 Duncan Avenue, Room B115
                            Bolling AFB, DC 20332-8050

Prepared by: Michael Miller
                      F&S Inc.
                      2801 Commerce Street
                      Blacksburg, VA 24062

Principal Investigator

F&S, Inc.

1. Introduction

The objective of this Phase I STTR program is to transfer the technology for Ionically Self-Assembled Monolayer (ISAM) nonlinear optical films to the development of advanced thin films that are easily fabricated at low cost and possess long-term stability as well as additional exceptional secondary material properties. The initial proof-of-concept demonstration has been achieved using an ionic polymer dye with a noncentrosymmetric chromophore, but the ISAM technique can be applied to create $\chi^{(2)}$ thin films from a wide variety of organic and polymeric structures.

2. Program Task Review

The technical tasks proposed by F&S as key to the development and commercialization of ISAM-processed $\chi^{(2)}$ waveguide device applications are summarized as follows.

Task 1 - Identify NLO chromophores and polymer dye molecules that together can give the fabricated ISAM thin films substantial $\chi^{(2)}$ response as well as long term stability and mechanical and thermal robustness. This builds on substantial Virginia Tech chemistry experience in ISAM design, synthesis and evaluation.

Task 2 - Develop the precursor *aqueous solution* chemistries required to obtain uniform suspensions of desired anions and cations in solution. This is based on recent ISAM research results with particles that are particularly difficult to process, such as TiO_2, Fe_3O_4, ZrO_2, phthalocyanines and polymer dyes in combination with high-performance polymers such as polyimides and polyamides. These results have been obtained with assistance from the NSF High Performance Polymer Center.

Task 3 - Fabricate ISAM NLO multi-micron thin films using existing ISAM fabrication facilities at Virginia Tech and developed facilities at F&S. The simple

ISAM fabrication process may be implemented using low cost dip processing equipment.

Task 4 - Reconfirm and quantitatively evaluate recent results indicating the existence of $\chi^{(2)}$ response by second harmonic generation (SHG) measurements using a fundamental wavelength of 1064 nm. A nonzero SHG signal indicates the required noncentrosymmetric ordering has been achieved in the ISAM thin film.

Task 5 - Quantitatively characterize the structural properties of the fabricated ISAM NLO films using materials analysis testing facilities, including XPS, SEM, Auger, ESCA microprobe and mechanical testing equipment. Such characterization will provide information for further optimization of ISAM NLO films and will evaluate the secondary materials properties of the films.

Task 6 - Evaluate the magnitude of the SHG response as a function of the number of deposited monolayers on the film. Uniform ordering with increased film thickness will be manifest as a quadratic dependence of the SHG signal on the number of layers.

Task 7 - Determine the orientation of the ISAM NLO chromophores by polarization-dependent SHG studies. Typical NLO chromophores have a single dominant tensor component of $\chi^{(2)}$ response along the long, donor-acceptor molecular axis.

Task 8 - Evaluate the long-term stability of the $\chi^{(2)}$ response of the ISAM NLO films. In contrast to the thermodynamically-unstable state of poled polymers, ISAM NLO films self-assemble into a stable configuration which should not decay over time.

Task 9 - Determine the critical parameters for optimization of ISAM NLO thin films and waveguide architectures for implementation in Phase II and for use in near-term commercial products. This includes selection of improved NLO

chromophores, identification of optimal counterion materials, and evaluation of methods of patterning waveguides.

3. Background

3.1 Nonlinear Optical Thin Films

In order to possess nonzero even-order nonlinear optical susceptibilities, a material must lack a center of inversion at the macroscopic level. As a result of the multitude of potential frequency conversion, optical modulation, and optical switching applications that stem from the $\chi^{(2)}$ second order susceptibility, several novel methods for creating noncentrosymmetric materials incorporating organic molecules with large β molecular susceptibilities have been developed over the past decade. These include electric field poled polymers, Langmuir-Blodgett films, and covalent self-assembled monolayer structures. This report concerns the first demonstration of a novel ionically self-assembled monolayer technique for the creation of noncentrosymmetric organic thin films with substantial $\chi^{(2)}$ values. The advantages of this technique include simple, rapid, inexpensive production and long-term stability of the induced $\chi^{(2)}$ without the need for additional processing such as electric field poling or chemical reactions.

3.2 Ionic Self-Assembly Process

Preparation of organic thin-films based on spontaneous molecular assembly is one of the powerful approaches to create novel supermolecular assemblies. Recently, Decher and co-workers extended the pioneering work of Iler *et al.* to a new preparative method of organizing thin-films by layer-by-layer adsorption of linear polyions. Alternate adsorption of a polycation and a polyanion is readily achieved by successive adsorption of polyelectrolytes on oppositely-charged surfaces. The general technique is characterized by several advantages including the simplicity of fabrication, the availability of a wide variety of water soluble polyions, and the molecular-level thickness of each formed monolayer.

Figure 1 shows the fundamental concept and simplified physical model behind the basic ionic self-assembled monolayer (ISAM) process. The substrate surface has been thoroughly cleaned, and charged through chemical processing. The charged substrate is then dipped into a solution containing water soluble "cation" polymer molecules. Because the polymer chain is flexible, it is free to orient its geometry so a relatively low energy configuration is achieved. Some functional groups along the polymer chain have localized positive charges so experience attractive forces toward the negative substrate, and the chain bends in response to those forces. The net negative charge of the substrate surface is thus partially masked from other positive functional groups along the polymer chain. Those groups feel a net force due to the fixed positive functional groups bonded to the substrate, so move to form a net positive charge distribution on the outermost surface of the coated substrate. Since the polymer layer is neutral, negative charges with relatively loose binding to the polymer network pair up with the positive ions. In this way, the total energy of the layer configuration is relatively low. Subsequent monolayers may be added in bilayer pairs by alternately dipping the substrate into polyionic solutions, to produce a multi-layer thin-film structure as shown. Nanoparticles, appropriately charged, such as fullerenes, metallofullerenes, and carbon nanotubes can also be substituted for the appropriate polymer layers in the process, thereby incorporating their functionality into the film layers.
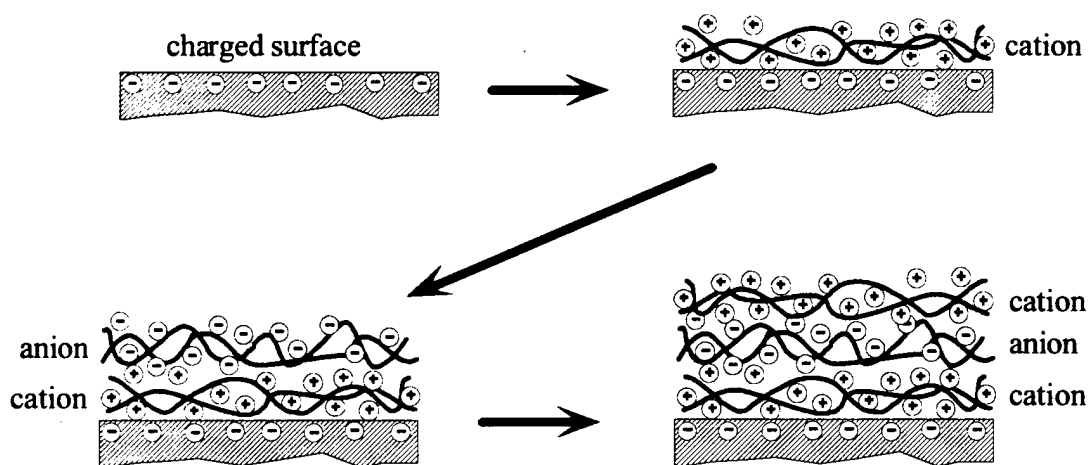
Figure 1. Basic ionic self-assembled multilayer (ISAM) process.

Polyelectrolyte self-assembly processing has specific advantages.

- **Excellent nanoscale molecular level uniformity** permits the fabrication of coatings with exceptional characteristics. Homogeneous mixtures of inorganic nanoparticles, **including fullerenes**, can be incorporated into the thin-films, and the ratio of polymer to nanoparticles controlled by adjusting bilayer thicknesses.

- **Surfaces with extremely complex geometrical shapes** may be coated uniformly due to the aqueous nature of the coating process. Ionic bonding of molecules in sequential layers inherently self-limits thickness and allows fabrication of very uniform coatings over the very large surfaces of space-based structural systems or the very small surfaces of optical or electronic components.

- **Synthesis is performed at room temperature and pressure.** Avoidance of high-temperature binder burnout processing means that polyelectrolyte coatings may be created on nearly any solid material substrate, including ceramics, plastics, metals (with proper surface treatment to allow charging), semiconductors or organic films, without degrading or destroying the substrate.

- **Capital equipment costs for basic fabrication are extremely low** (the cost of large liquid containers), may be upscaled in size and volume, and may be easily automated.

- **Capability for thick multi-layer fabrication** is allowed due to the uniformity of each layer and the avoidance of geometrical defects caused by conventional covalent bonding-based self-assembled monolayer approaches that allow deposition of only two or three superimposed layers. F&S-sponsored research at Virginia Tech has demonstrated the synthesis of more than 2000 ISAM layers with good surface morphology. Multi-layer structures allow the possibility of incorporating multiple functions into a single coating.

- **Broad range of layer functionality** is possible through incorporation of a wide range of inorganic nanoparticles to control of the electronic, conductive, optical, magnetic, thermal and mechanical properties. High performance polymers may allow excellent thermal stability, mechanical properties and processability.

- **Environmentally friendly process.** Fabrication uses aqueous polyelectrolyte solutions and no volatile organic compounds (VOCs).

3.3 Initial ISAM-Fabricated NLO Thin-Films

The ISAM thin films are grown monolayer by monolayer by first immersing an initially charged substrate into an aqueous solution containing an oppositely charged polyelectrolyte. This is followed by rinsing and then by immersion of the substrate into a second polyelectrolyte that is of opposite charge to the first. The dipping process can be repeated as many times as desired until a film with the chosen number of bilayers has been produced. The ISAM $\chi^{(2)}$ films were deposited on glass microscope slide substrates. The substrates were first prepared by cleaning with "piranha solution," a 30:70 mixture of 30% hydrogen peroxide and concentrated sulfuric acid at 80° C for one hour followed by extensive rinsing with ultrapure water obtained from a Barnstead Nanopure III system, a final rinsing with absolute ethanol, and drying in an oven. The substrates thus cleaned were then dipped in a solution of 2% N-2-(2-aminoethyl)-3-aminopropyltrimethoxysilane (APS) in pure methanol for 15 hours. Afterward, the substrates were ultrasonically agitated for 30 minutes each in methanol and water. Finally, they were extensively rinsed with ultrapure water to remove residual APS and dried. Such an APS-modified surface is positively charged.

Noncentrosymmetric, ISAM $\chi^{(2)}$ films have been produced using two different polyanions: the polymeric dyes Poly S-119 (see inset of Figure 2), which consists of a poly(vinylamine) backbone with an ionic azo dye chromophore (from Sigma), and poly{1-[4-(3-carboxy-4-hydroxyphenylazo)benzensulfonamido]-1,2-ethanediyl, sodium salt} (PCBS, from Aldrich). While either Poly S-119 or PCBS served as the polyanion for the ISAM fabrication, poly(allylamine hydrochloride) (PAH), which has no $\chi^{(2)}$ response, was used for the polycation. For these materials, we have found through measurements of absorbance and of film thickness (by ellipsometry) as a function of immersion time that the formation of each monolayer is complete in less than twenty seconds of immersion in the polyelectrolyte. This allows the rapid buildup of self-assembled, multilayer films. Furthermore, our measurements of second harmonic generation demonstrate that the strong internal electric fields of the ionic layers lead to alignment of the polar NLO chromophores, and the resulting noncentrosymmetric films

possess substantial $\chi^{(2)}$ values.

Figure 2 shows the absorption spectrum of an ISAM film with 100 bilayers of Poly S-119/PAH deposited on a single side of the glass substrate. The film is orange in color and exhibits exceptional homogeneity and lack of scattering. In Figure 3, the absorbance at 500 nm of several films is plotted versus the number of bilayers. The linear growth of absorbance with the number of deposited layers illustrates the homogeneous deposition of the polymer dye with each successive layer. The film thickness, determined by ellipsometry, as a function of the number of deposited bilayers for Poly S-119 is shown in Figure 4. Each bilayer is found to have a thickness of 1.2 nm. We have previously prepared ISAM films of other materials consisting of greater than one thousand bilayers.

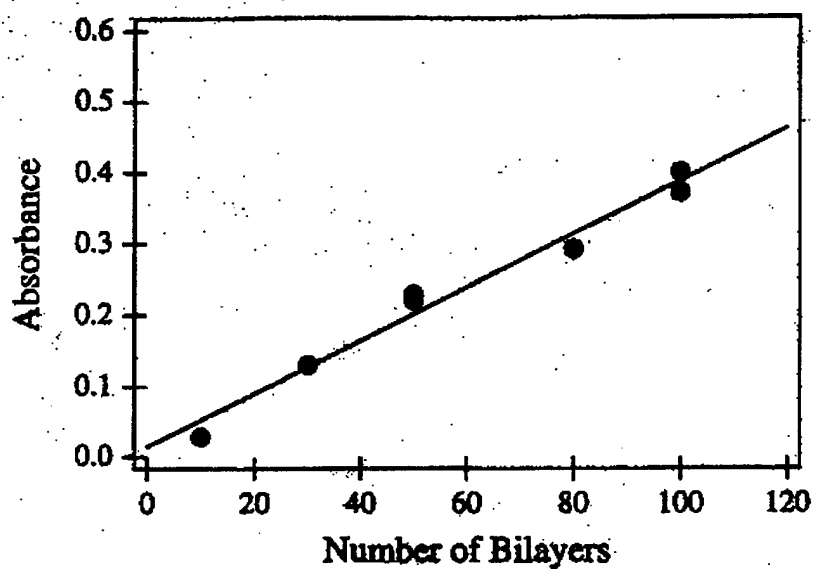**Figure 2. Absorption spectrum of a Poly S-119/PAH ISAM film with 100 bilayers.**

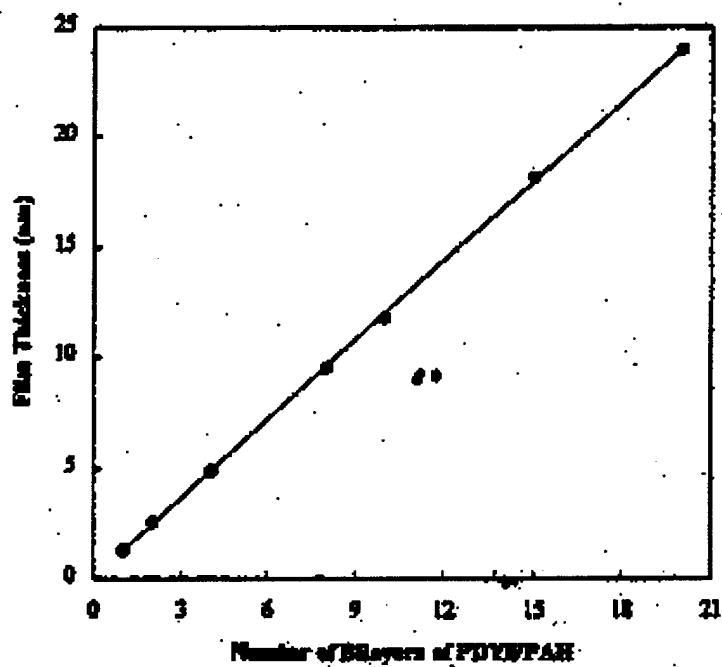**Figure 3.** Absorbance at 500 nm as a function of the number of Poly S-119/PAH bilayers.

Figure 4. Film thickness as a function of the number of Poly S-119/PAH bilayers.

3.4 Second Harmonic Generation Measurements of ISAM Films

The SHG experiments were carried out using both the 1064 nm fundamental wavelength of a Q-switched Nd:YAG laser and the 1200 nm output from a broadband, BBO optical parametric oscillator (OPO). The OPO is pumped by the 355 nm third harmonic of the Nd:YAG and is continuously tunable from 400 to 2500 nm. The 504 nm OPO signal beam is removed from the 1200 nm idler beam using a 700 nm long-pass filter. The incident intensity and polarization on the sample are controlled by a pair of Glan-Laser polarizing prisms. The fundamental beam is weakly focused onto the sample and a 532 or 600 nm spike filter is employed to ensure that the photomultiplier tube measures only the intensity of the second harmonic light. The incident fundamental intensity into the sample is measured using a beamsplitter and photodiode.

3.5 Poly S-119/PAH ISAM Films

Since the Poly S-119 films are strongly absorbing at 532 nm, we concentrate here primarily on the measurements using the 1200 nm fundamental wavelength. Figure 5 illustrates the dependence of the SHG signal intensity as a function of the incident fundamental intensity for a single-sided, 68 bilayer Poly S-119 film. The film is rotated 45° away from normal incidence about the vertical axis, and the incident light is p-polarized. The solid curve is a best fit to the data of the form $I_{2\omega} = A(I_{\omega})^{b}$, where $I_{2\omega}$ and I_{ω} are the second harmonic and fundamental intensities, respectively. The fit yields a value of $b = 2.02$, in excellent agreement with the expected quadratic dependence on fundamental intensity.

When the ISAM $\chi^{(2)}$ films are rotated to normal incidence, negligible SHG is observed. This is consistent with the expectation that the alignment of the chromophores occurs perpendicular to the substrate. Furthermore, when the sample is oriented at 45° to normal incidence and the polarization of the fundamental beam is varied, the SHG intensity is observed to smoothly vary from a maximum for horizontal, p-polarized light to a minimum for vertical, s-polarized light, again consistent with dipolar orientation perpendicular to the substrate
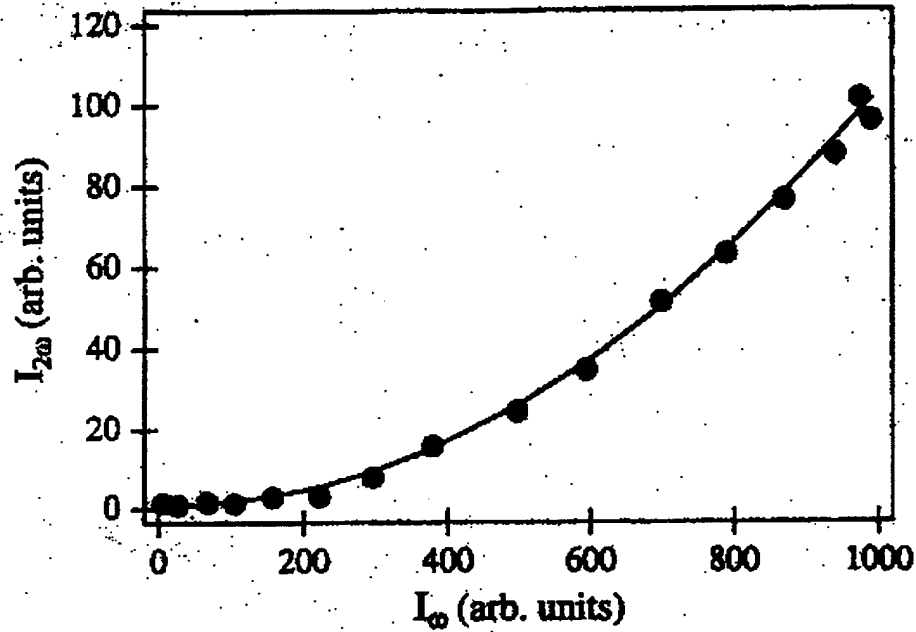
Figure 5. Dependence of the second harmonic intensity at 600 nm on the fundamental intensity at 1200 nm for a 68 bilayer Poly S119-PAH film.

The dependence of the second harmonic intensity on film thickness and $\chi^{(2)}$ is given by

$$I_{2\omega} \propto (l_c \chi_{eff}^{(2)})^2 \sin^2\left(\frac{\pi l}{2l_c}\right)$$

(1)

where l is the sample thickness, $l_c = \lambda/[4(n^{2\omega}-n^{\omega})]$ is the coherence length, and $\chi_{eff}^{(2)}$ is the effective susceptibility determined by the sample geometry and the nonzero components of the $\chi^{(2)}$ tensor. In the limit that the sample thickness is much less than the coherence length, the second harmonic intensity is quadratic in the film thickness. Since the films studied here are in the $l \ll l_c$ limit, the SHG intensity is expected to grow quadratically with the number of bilayers. In Figure 6, $(I_{2\omega})^{1/2}$ is plotted versus the number of bilayers for several Poly S-119/PAH films. The data are seen to be in excellent agreement with the quadratic dependence. This demonstrates that the orientation of the chromophores is the same for each successive layer. If the degree of orientation was decreased for the

latter deposited layers, the SHG intensity would yield a subquadratic dependence on the number of bilayers.
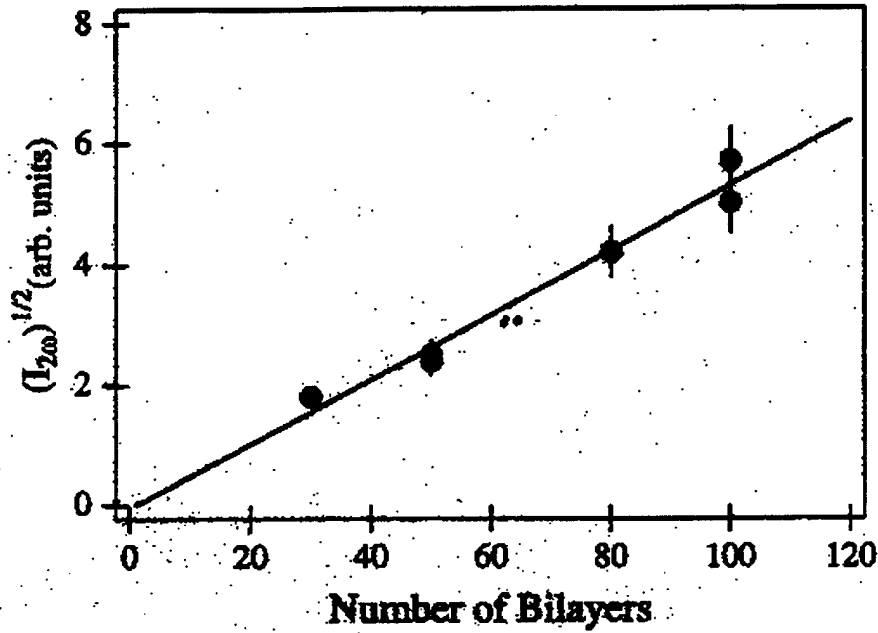

Figure 6. Square root of the measured second harmonic intensity as a function of the number of bilayers for Poly S-119/PAH.

Our polarization-dependence measurements indicate that the dipolar orientation of the chromophores is perpendicular to the substrate. Taking this direction as z and assuming Kleinman symmetry, we have $\chi_{xzx}^{(2)} = \chi_{zxx}^{(2)} = \chi_{yzy}^{(2)} = \chi_{zyy}^{(2)} = (1/3)\chi_{zzz}^{(2)}$. With the sample rotated from normal incidence at an angle θ about the vertical axis and using p-polarized fundamental and second harmonic light, the effective susceptibility for the ISAM film is

$$\chi_{eff}^{(2)} = (3\chi_{zxx}^{(2)} \sin\theta \cos^2\theta + \chi_{zzz}^{(2)} \sin^3\theta) \qquad (2)$$

$\chi_{zzz}^{(2)}$ of the ISAM films is determined from eqns. (1) and (2) by comparison to Maker fringes generated using the $\chi_{xxx}^{(2)}$ (corresponding to d_{11}) coefficient of a quartz wedge. The $\chi_{zzz}^{(2)}$ value for Poly S-119/PAH is found to be 0.70 times the value of quartz, or 0.67×10^{-9} esu. Importantly,the first ISAM $\chi^{(2)}$ films that we created have exhibited no

measurable decay of $\chi_{zz}^{(2)}$ over a period of more than six months.

3.6 PCBS/PAH ISAM Films

ISAM $\chi^{(2)}$ films have also been fabricated using PCBS as the active polyanion layer and PAH as the passive polycation layer. The absorption spectrum for a film with 100 bilayers is shown in Figure 7. The films are yellow in color and again exhibit exceptional homogeneity. As in the case of Poly S-119/PAH, the PCBS/PAH films exhibit a linear dependence of the absorbance and a quadratic dependence of the second harmonic intensity on the number of deposited bilayers. In addition, we have performed detailed polarization dependence measurements on the 100 bilayer PCBS/PAH film. For orientation of the chromophore dipoles perpendicular to the substrate, it can be shown that there is no s-polarized component of the second harmonic intensity when the fundamental beam is strictly s- or p-polarized. Using a p-polarized incident fundamental beam with the sample rotated at 45 $^{\mathrm{O}}$ from normal incidence, the second harmonic intensity was measured as a function of the angle of a polarizer placed in front of the PMT. The results are illustrated in Figure 8, where 90 $^{\mathrm{O}}$ corresponds to a horizontal, p-polarized second harmonic signal. The data confirm the lack of a vertical, s-polarized component to the second harmonic signal and are in excellent agreement with the expected $\sin^2 \phi$ dependence on the polarizer angle.
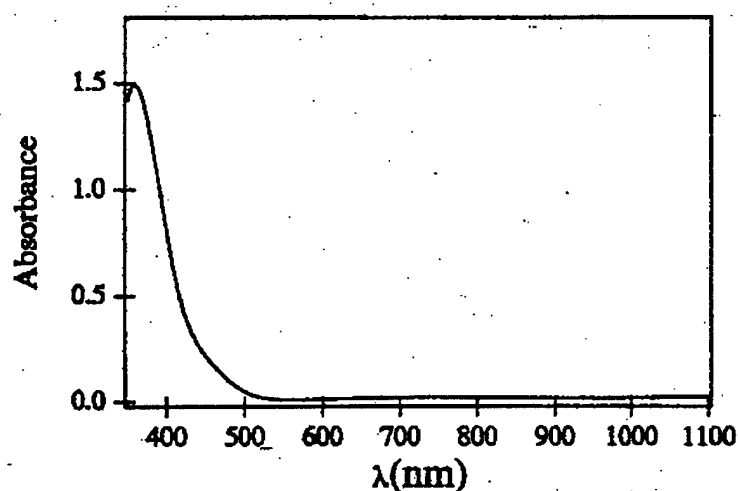

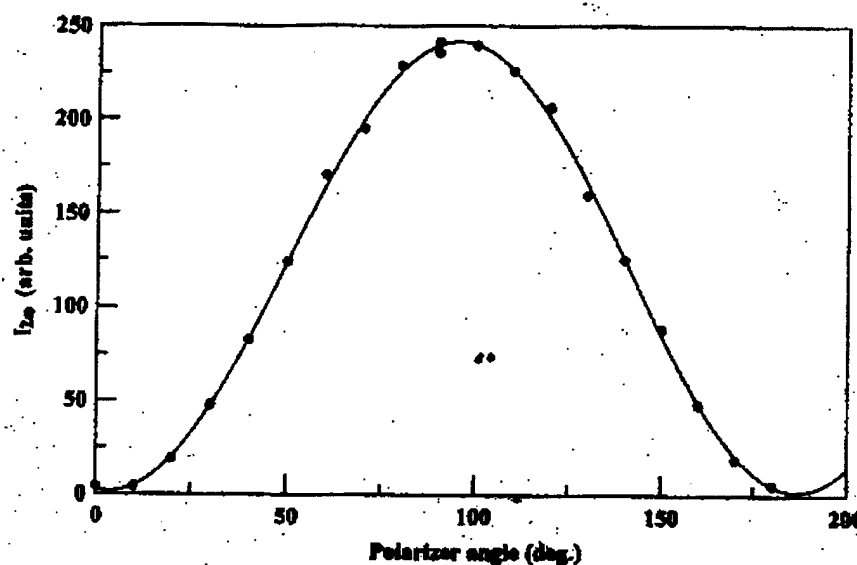**Figure 7. Absorption spectrum of 100 bilayer PCBS/PAH ISAM film.**

Figure 8. Polarization of the second harmonic intensity for p-polarized incident fundamental beam.

We have also carried out a preliminary study on the thermal stability of $\chi^{(2)}$ in the PS-119 ISAM film. The sample was first heated to 100° C in 25° increments. The magnitude of $\chi^{(2)}$ at each temperature was determined by fitting the data for $I^{2\omega}$ vs. I^ω as in Figure 5 and comparing to the data obtained at room temperature immediately prior to heating. The relative $\chi^{(2)}$ value as a function of time is shown in Figure 9. The second, third, and fourth data points correspond to temperatures of 50, 75 and 100° C, respectively, as the sample temperature was raised over the course of three hours. The magnitude of $\chi^{(2)}$ was observed to decrease by roughly 20% over this time period. The sample was then maintained at 100° C for more than forty hours. Very little further decay was observed in $\chi^{(2)}$ during this extended heating period. Following more than 40 hours at 100° C, the sample maintained >70% of its initial $\chi^{(2)}$ value.

3.7 Developments in Nanoparticle, Precursor and Thin-Film Synthesis

We have observed nonlinear optical (NLO) behavior in polymer/organic dye ISAM thin-films, using commercially available dye molecules, P-S119 (Sigma) and PCBS (Aldrich), as well as newly synthesized polymer dyes, Polydye1 and Polydye2. During this

program we have synthesized several new NLO polymers. The UV-Vis spectra of aqueous solutions of these polymers are shown in Figure 9. Results of second harmonic generation experiments using these Polydyes are discussed in following sections.
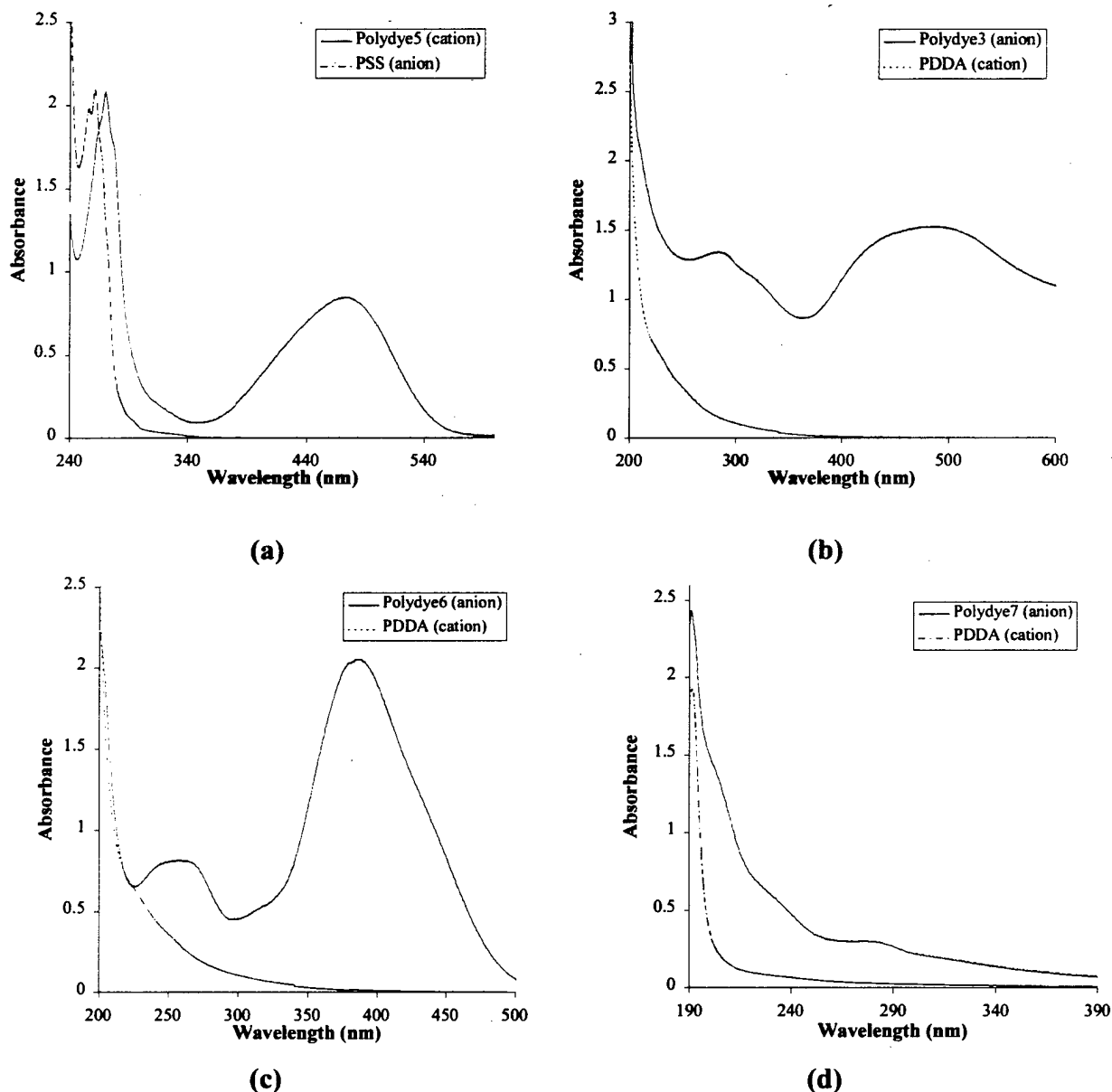

(a)

(b)

(c)

(d)

Figure 9. UV-Vis Spectra of (a) Polydye3; (b) Polydye5; (c) Polydye6; and (d) Polydye7 Aqueous Solutions.

Multi-layer thin-films of Polydye3, Polydye6 and Polydye7 were self-assembled on glass and quartz substrates with polydiallyldimethylammonium chloride (PDDA) as the passive polycation layer.

UV-Vis spectroscopy was used to identify the absorption and transmission characteristics of the NLO thin-films as well as to quantify the growth of the multilayer structures. For example, optical absorbance spectra measured during the growth of a Polydye3 film on a modified glass substrate is shown in Figure 10. We are currently investigating variations of the solution chemistry to reduce optical scattering from the thin-films.

The UV-Vis spectra of Polydye6 and Polydye7 are shown in Figure 11 and Figure 12. The absorbance peaks are located at 380 and 208 nm, respectively. The inset in Figure 12 shows the linear growth of Polydye7, which has an average optical density of 0.048 (at 208 nm) per bilayer. For each spectrum, three sets of UV-Vis data were obtained at different locations on each specimen. The maximum differences between data at different locations is at most a few percent, indicating excellent uniformity of the films. The ellipsometry data for Polydye7 is shown in Figure 6, yielding an average thickness of 31 Å per bilayer.
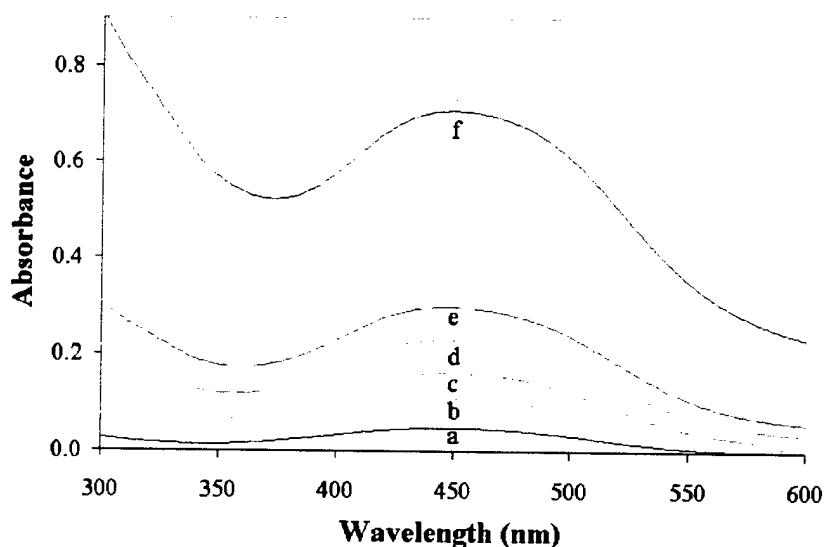

Figure 10. UV-Vis Absorbance of Polydye3 Thin-Films [(a) 3 bilayers; (b) 6 bilayers; (c) 9 bilayers; (d) 12 bilayers; (e) 15 bilayers; (f) 30 bilayers].
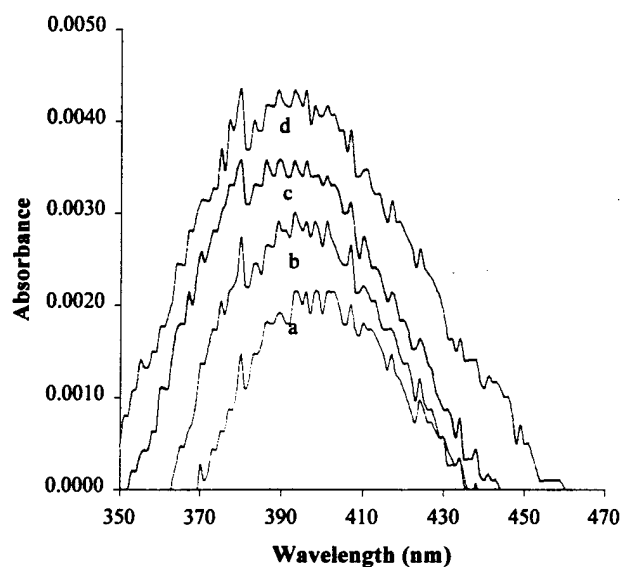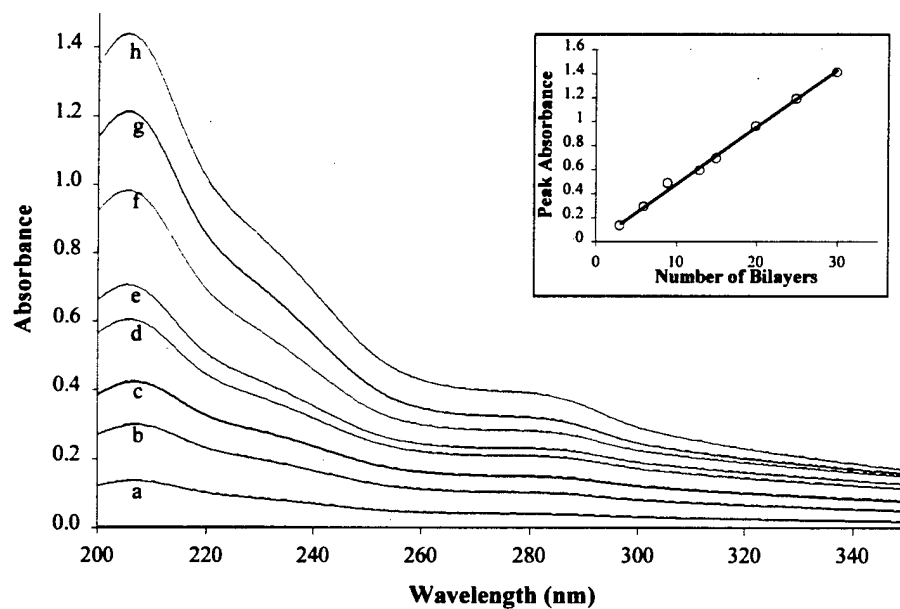
Figure 11. UV-Vis Absorbance of Polydye6 Thin-Films [(a) 5 bilayers; (b) 10 bilayers; (c) 15 bilayers; (d) 20 bilayers].

Figure 12. UV-Vis Absorbance of Polydye7 Thin-Films [(a) 3 Bilayers; (b) 6 Bilayers; (c) 9 Bilayers; (d) 13 Bilayers; (e) 15 Bilayers; (f) 20 Bilayers; (g) 25 Bilayers; (h) 30 Bilayers] with Inset Showing the Linear Relationship Between Absorbance at 208 nm and the Number of Bilayers Assembled.
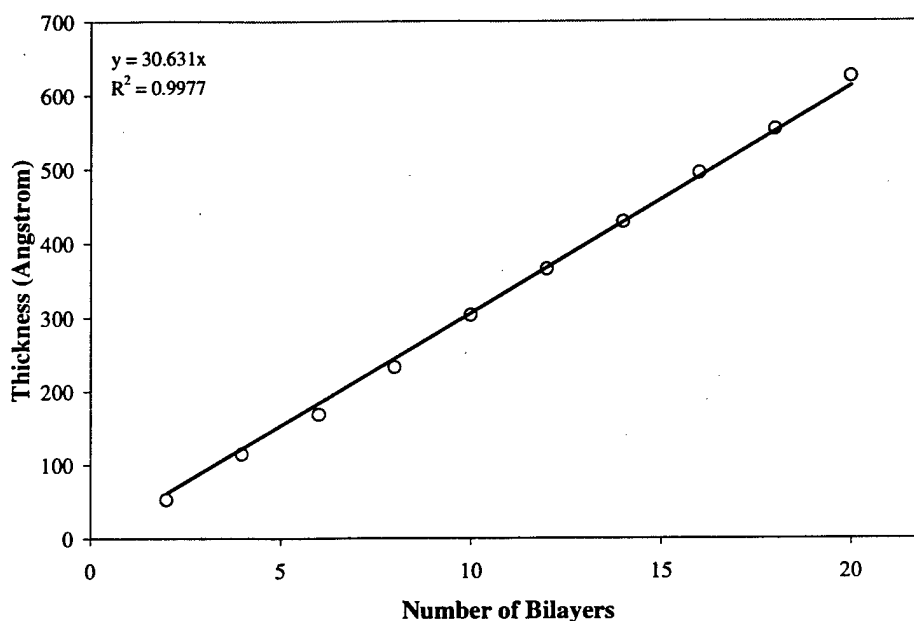
$$y = 30.631x$$
$$R^2 = 0.9977$$

Figure 13. Polydye7/PDDA ISAM Film Thickness.

3.8 Fluorescence

Thin-film emission characteristics have important implications for optical and optoelectronic devices. As examples, the fluorescence spectra of Polydye2 and Polydye4 ISAM films are shown in Figure 14 and Figure 15. For comparison, the emission spectra of the original Polydye solutions are shown on the same axes. The emission characteristics of other Polydyes will be determined in the future.

3.9 Polydye1 Improvements

We have reported a $\chi^{(2)}$ value six times that of commercially available Poly S-119 for the first polymer we synthesized, Polydye1. However, the initially fabricated films exhibited some self-assembly problems, resulting in inhomogeneities. Modification of Polydye1 solution chemistry has resulted in the fabrication of films that are exceptionally uniform. The UV-Vis spectra for a Polydye1 ISAM thin-film with increasing numbers of bilayers is shown in Figure 16; Figure 17 illustrates the increase in absorbance peaks with the

addition of each bilayer. The nonlinear film growth indicated by the quadratic increase in optical absorbance is confirmed by ellipsometry data, illustrated in Figure 18.
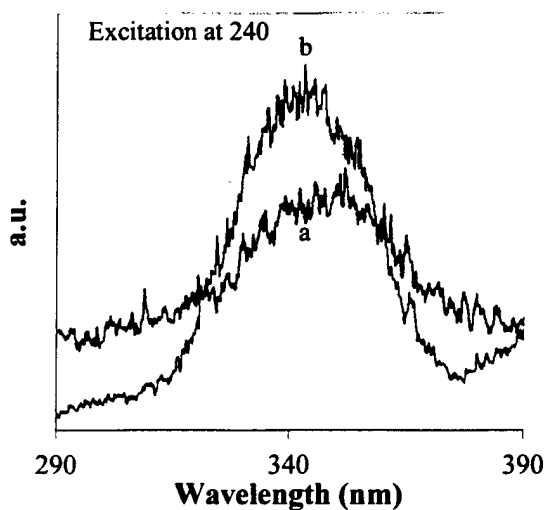

Figure 14. Fluorescence Spectra: (a) ISAM Thin-Film of Polydye2 on Glass; (b) Aqueous Polydye2 Solution.
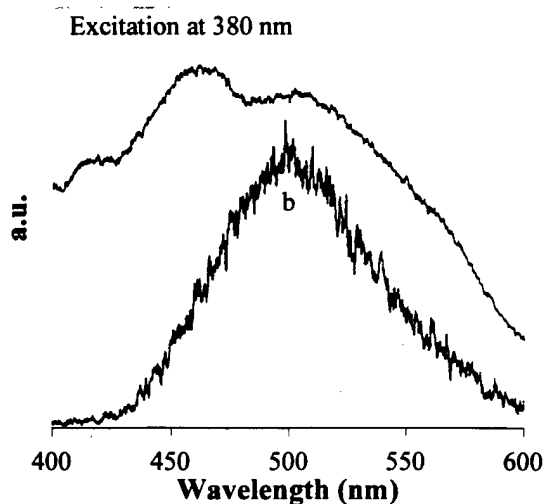
Figure 15. Fluorescence Spectra: (a) ISAM Thin-Film of Polydye4 on Glass; (b) Aqueous Polydye4 Solution.

The thickness of each bilayer increases with the addition of each successive bilayer; the overall film thickness increases quadratically. To investigate the origin of this interesting phenomenon, the films were further evaluated using the scanning electron microscope. 3 bilayer, 10 bilayer and 18 bilayer films were fabricated on single crystal silicon substrates. Visual inspection of the SEM micrographs revealed not only uniformity across each film surface, but also decreasing grain size with increasing numbers of bilayers. This indicates a change in the arrangement and alignment of the polymers in each bilayer.

3.10 Developments in $\chi^{(2)}$ Measurements in ISAM Thin-Films

We have continued to design and synthesize novel polymers that are mutually compatible with the ISAM deposition process and with high NLO response. A total of seven new Polydye polymers have been synthesized and deposited since the inception of this

project. Figure 19 shows a comparison of the SHG signal from a 30 bilayer Polydye3 sample and the 68 bilayer Poly S-119 reference standard. By comparison to the Maker fringes generated in a quartz wedge, the 68 bilayer Poly S-119 ISAM film was determined to have a $\chi^{(2)}$ value of 1.34×10^{-9} esu. This film is then used as the reference standard, and the $\chi^{(2)}$ of other ISAM films is determined with respect to this film using Eq. (1). By fitting the data of Figure 19, the $\chi^{(2)}$ of the Polydye3 film was determined to by 0.91×10^{-9} esu, or 68% of the Poly S-119 $\chi^{(2)}$.

Polydye1 film was shown to have a $\chi^{(2)}$ value six times larger than that of Poly S-119. The film quality of the Polydye1 sample was, however, less homogeneous than that of other ISAM films resulting in substantial scattering loss. Through modification of the deposition parameters, we have successfully deposited Polydye1 films that exhibit the exceptional homogeneity that is typical of ISAM films. SHG data for a new, homogeneous, 15 bilayer Polydye1 film is shown in Figure 20 in comparison with Poly S-119. Although the total SHG signal is less for the Polydye1 film, the $\chi^{(2)}$ obtained, accounting for difference in film thickness according to Eq. (1), is 3.26×10^{-9} esu, or 2.4 times larger than that of Poly S-119. This $\chi^{(2)}$ is 2.6 times less than that measured in the inhomogeneous Polydye1 film. This decrease can be understood from the absorption spectra of the two films. The peak absorbance at 450 nm of the first, inhomogeneous film is 0.14 while the peak absorbance of the homogenous film is 0.03. This indicates a decrease in chromophore density by a factor of 4.5 in the homogeneous film. The homogeneous film, therefore, does make a more effective use of the chromophore when the lower chromophore density is accounted for.
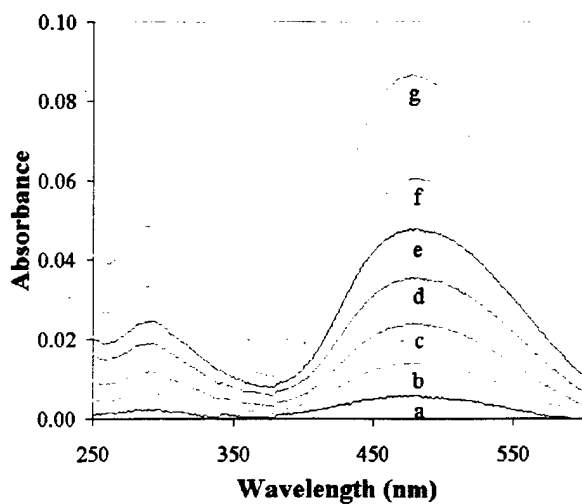
Figure 16. UV-Vis Absorbance of Polydye1 Thin-Films [(a) 2 Bilayers; (b) 4 Bilayers; (c) 6 Bilayers; (d) 8 Bilayers; (e) 10 Bilayers; (f) 12 Bilayers; (g) 16 Bilayers].
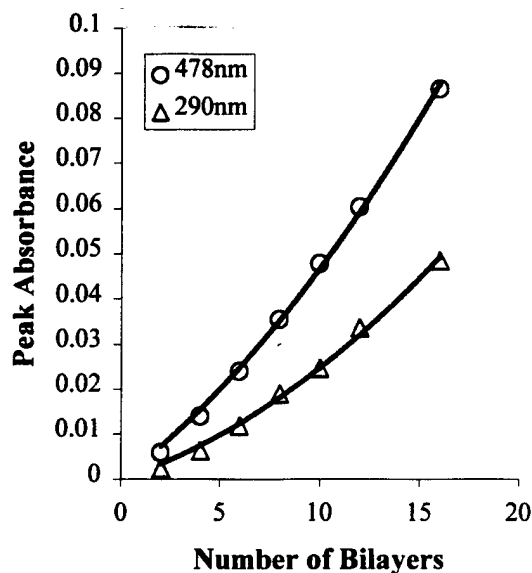
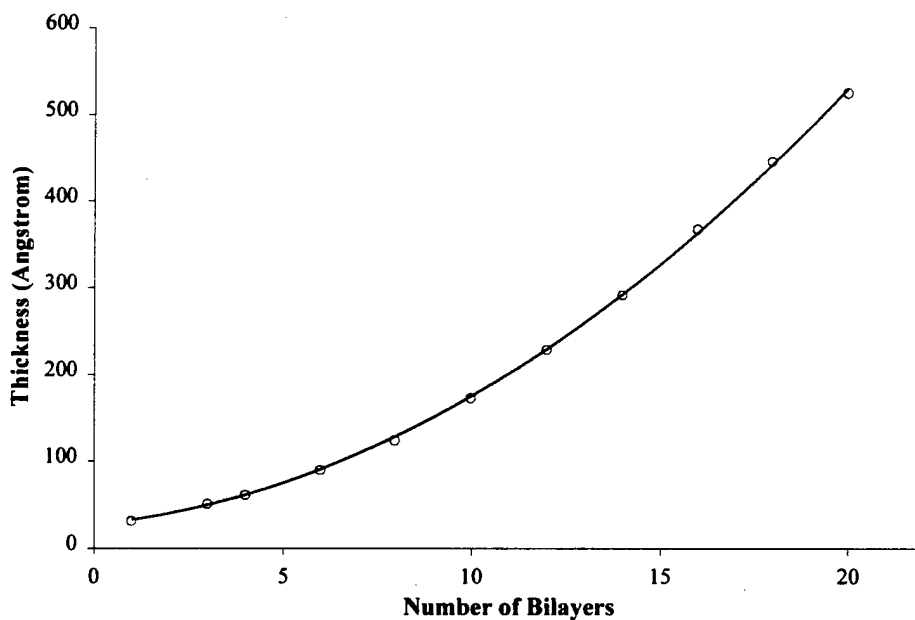**Figure 17.** Quadratic Relationship Between Absorbance at 478 nm and 290 nm and the Number of Bilayers Assembled.
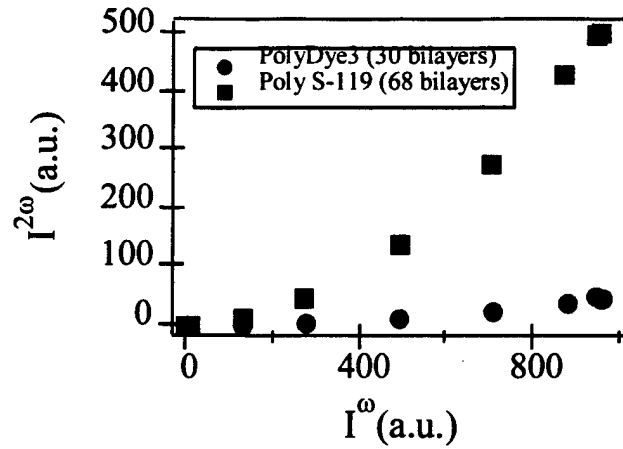

Figure 18. Polydye1/PDDA ISAM Film Thickness.

**Figure 19. Comparison of SHG signal for 30 Bilayer Polydye 3 and
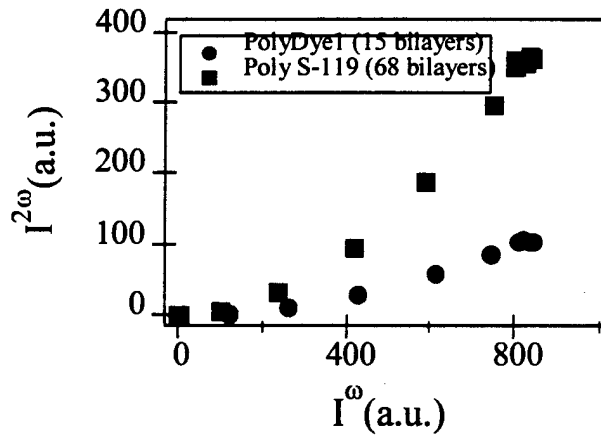68 Bilayer Poly S-119 ISAM Films.**

**Figure 20. Comparison of SHG Signal for 15 Bilayer Polydye1 and
68 Bilayer Poly S-119 ISAM Films.**

We are beginning to develop a fairly extensive database of $\chi^{(2)}$ values for new Polydye polymer ISAM films. This has allowed us to determine an improved set of design criteria concerning the simultaneous optimization of $\chi^{(2)}$ and compatibility with the ISAM fabrication technique. These results are now guiding our current synthesis and deposition work.

3.11 Characterization of Thermal Stability of ISAM NLO Thin-Films

To further investigate the thermal stability of the $\chi^{(2)}$ response in ISAM NLO films, we measured the second harmonic generation in a Poly S-119/PAH 100 bilayer ISAM film as the temperature was raised to 150° C for greater than fifteen hours. Remarkable behavior was observed. While the $\chi^{(2)}$ value was found to decrease to 75% of the initial value as the temperature was raised, it exhibited outstanding stability as the temperature was maintained at 150° C. Most strikingly, as the sample was cooled, $\chi^{(2)}$ again increased. While we believe we understand the origin of this effect, it bears deeper investigation.

The SHG experiments were carried out using the 1200 nm output from a broadband, BBO optical parametric oscillator (OPO). The OPO is pumped by the 355 nm third harmonic of the Nd:YAG and is continuously tunable from 400 to 2500 nm. The 504 nm OPO signal beam is removed from the 1200 nm idler beam using a 700 nm long-pass filter. The incident intensity and polarization on the sample are controlled by a pair of Glan-Laser polarizing prisms. The fundamental beam is weakly focused onto the sample and a 532 or 600 nm spike filter is employed to ensure that the photomultiplier tube measures only the intensity of the second harmonic light. The incident fundamental intensity into the sample is measured using a beamsplitter and photodiode. For the temperature stability studies, the sample is contained in a programmable heating cell that has entrance and exit ports for optical access. The temperature is measured by two thermocouple probes placed in the top and bottom heating plates, respectively.

The Poly S-119 sample was heated to 150° C over the course of three hours. The temperature was maintained at the intermediate values of 50 and 100° C long enough to allow measurement of the second harmonic intensity at $\lambda=600$ nm as a function of the incident fundamental intensity at 1200 nm. Figure 21 shows data at 23, 50, 100, and 150° C as the sample was heated. The second harmonic intensity was observed to decrease monotonically as the temperature was raised. The experimental data were found in all cases to exhibit excellent quadratic dependence of the second harmonic intensity on
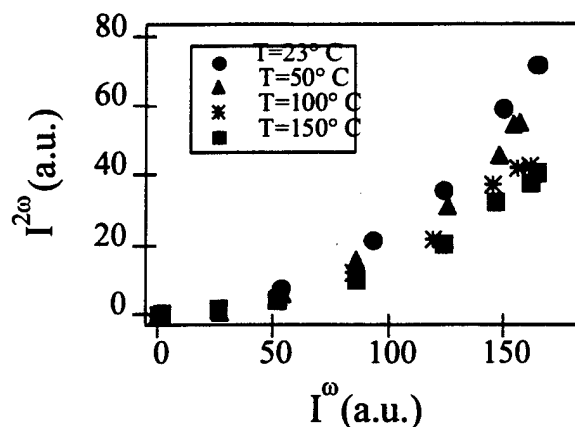
the fundamental intensity.

Figure 21. Second Harmonic Intensity as a Function of Incident Fundamental Intensity for Poly S-119/PAH ISAM Film as the Temperature is Increased to 150° C.

Once the temperature stabilized at 150° C, the sample was maintained at this temperature for fifteen hours. The second harmonic intensity was measured several times during this interval. SHG data is shown in Figure 22 for the initial time (t=0) at 150° C as well as 3.2, 5.6, and 15.3 hours after the temperature had reached 150° C. Nearly identical curves for the SHG signal were observed throughout this time period. It is clear that the $\chi^{(2)}$ response of the sample exhibited exceptional stability at this elevated temperature for greater than fifteen hours.
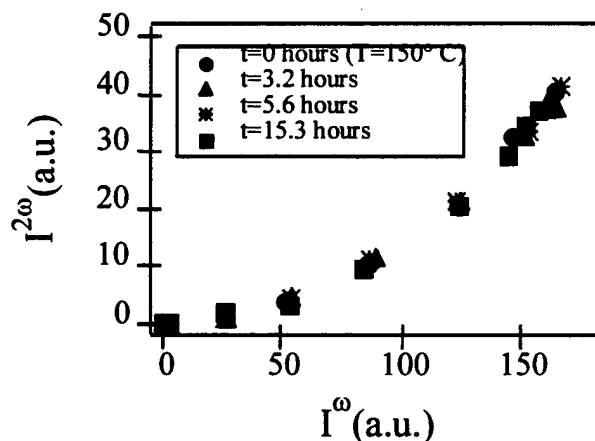

Figure 22. Second Harmonic Intensity as a Function of Incident Fundamental Intensity for Poly S-119/PAH ISAM Film as the Temperature is Maintained at 150° C for 15 Hours.
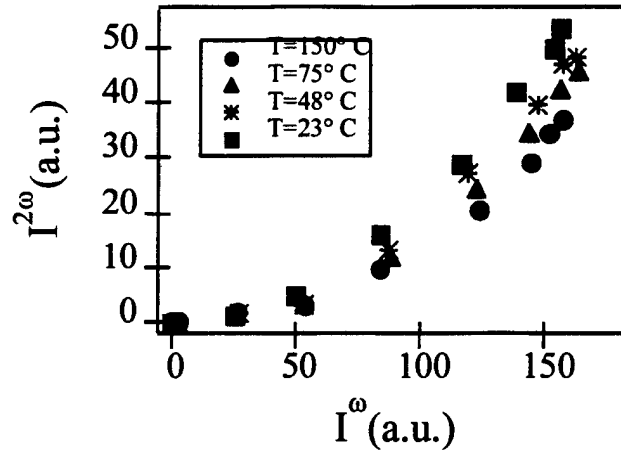
Figure 23. Second Harmonic Intensity as a Function of Incident Fundamental Intensity for Poly S-119/PAH ISAM Film as the Temperature is Cooled From 150° C.

The data were fit to the expression $I^{2\omega}=A(I^{\omega})^2$. Since the thickness of the ISAM films is much less than the second harmonic coherence length, the observed second harmonic intensity increases quadratically with the thickness of the film. In this limit, the $\chi^{(2)}$ value is determined by

$$\chi^{(2)} = \chi_{ref}^{(2)} \sqrt{\frac{A}{A_{ref}}} \frac{l_{ref}}{l} \tag{3}$$

where A is the coefficient of the fit to the second harmonic intensity as a function of fundamental intensity and l is the path length through the sample (thickness). The $\chi^{(2)}$ value for each time and temperature was determined relative to the $\chi^{(2)}$ of the sample prior to heating under the assumption that the film thickness was the same in all cases. As described below, it is believed that the film thickness in fact decreases as the temperature is elevated. The thickness was not quantitatively evaluated as a function of temperature, however. The effect of the constant thickness assumption will be further discussed below. The $\chi^{(2)}$ value relative to the initial value is plotted as a function of temperature in Figure 24. Measurements taken as the temperature was increased are represented by circles and those taken as the temperature was decreased are represented

by squares. As the temperature is raised to 150° C, $\chi^{(2)}$ is reduced by 25% of its initial value. During the fifteen hours the sample is maintained at 150° C, $\chi^{(2)}$ remains constant at 75% of the initial value. As the sample is cooled, the $\chi^{(2)}$ value increases to a final value that is 91% of the value observed prior to heating. Thus, the full temperature cycle results in a loss of only 9% of the $\chi^{(2)}$ response.
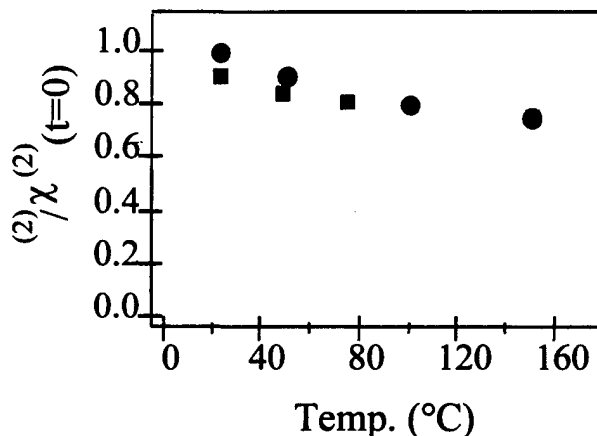

Figure 24. Relative $\chi^{(2)}$ Value as Function of Temperature Under the Assumption of Constant Thickness.

Decher and co-workers have reported using small angle x-ray scattering that the total thickness of an ISAM film is reduced as the temperature is increased [10]. The film thickness was observed to be restored nearly to its initial value when the film was cooled back to room temperature. Y. Liu has previously measured the contact angle of a water droplet on ISAM films as a function of temperature and found that the contact angle was increased as the temperature was raised [11]. The contact angle returned to its initial value following cooling of the sample. Since the contact angle measures the wettability of the surface, the results were interpreted as a decrease in the water content of the film at elevated temperatures that is accompanied by a decreased film thickness. As the temperature is decreased water is reabsorbed, and the film swells to its original thickness.

The second harmonic generation data can be explained within this model as follows. As the ISAM film is heated, water is driven out of the film resulting in a decrease in film

thickness. The compaction of the film is accompanied by an increased average tilt angle of the NLO chromophore with respect to the film normal that leads to a decreased $\chi^{(2)}$ value. Furthermore, since the film thickness is decreased, the assumption of constant thickness used to determine the relative $\chi^{(2)}$ values over-estimates the actual decrease in $\chi^{(2)}$. As the temperature is raised to 150° C, the actual decrease in $\chi^{(2)}$ is somewhat less than 25%.

The increased SHG signal that is observed as the sample cools is believed to be due to the reabsorption of water into the film. This is accompanied by an increase in the film thickness and a decrease in the average tilt angle of the NLO chromophore with respect to the film normal. Since the final SHG signal after the sample has completely cooled is still slightly less than the initial value, it is supposed that either the film thickness or the tilt angle are not fully restored. Ellipsometric and SHG polarization-dependence measurements will be made to evaluate these hypotheses.

3.12 Determination of Electro-Optic Coefficient in ISAM Thin-Films

Two 50 bilayer films were self-assembled on ITO-coated glass substrates using both a commercially available dye and a Polydye and sent to Professor Jeong Weon Wu at Ewha Womans University in Seoul, Korea. Professor Wu will perform electro-optic measurements on the films, and the results are expected to be available in the next report period. The UV-Vis absorbance spectra of these specimens are shown in Figure 25 and Figure 26. Both use polydiallyldimethylammonium chloride (PDDA) as the passive polycation layer.

4. Discussion of Product Application/Commercialization

F&S has held discussions of potential commercialization of NLO materials and devices based on such materials with several companies. These include TACAN and Lockheed-Martin Palo Alto. TACAN is a major U.S. manufacturer of electro-optic modulators used in the cable television industry, and has expressed interest in testing ISAM-based EO devices. Lockheed-Martin is a major developer and user of electro-optic materials and

devices for space system applications. Subcontract PI Professor Heflin visited the Lockheed Martin Advanced Technology Center at the invitation of Drs. Jar-Mo Chen and Susan Ermer to give a seminar on the development of $\chi^{(2)}$ materials using the ISAM technique. LM has indicated interest in obtaining materials for their analysis and testing.
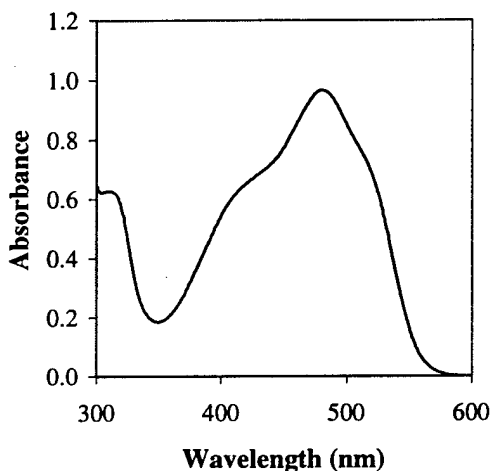
Figure 25. UV-Vis Absorbance of 50 Bilayer Poly S-119 Thin-Film Used for Electro-Optic Coefficient Measurements.
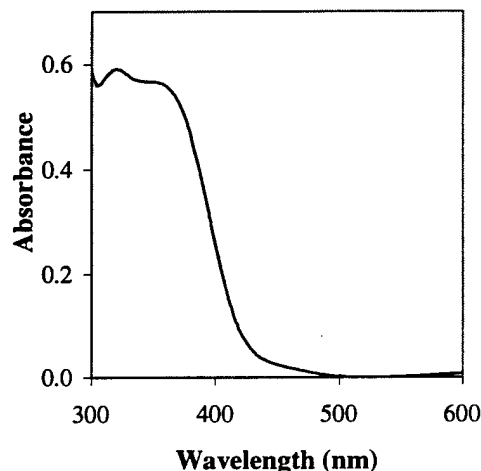
Figure 26. UV-Vis Absorbance of 50 Bilayer Polydye4 Thin-Film Used for Electro-Optic Coefficient Measurements.

5. References

[1] Y. Liu, A. Wang and R. Claus, "Molecular Self-Assembly of TiO_2-Polymer Nanocomposite Films," accepted for publication, *J. Physical Chemistry*, March or April issue, 1997.

[2] Y. Liu, A. Wang and R. Claus, "Layer-by-Layer Molecular Assembly of Nanoscale Fe_3O_4 Particles and Polyimide on Silicon and Silica Surfaces," Proc. MRS Conference, May 1997.

[3] Y. Liu, A. Wang and R. Claus, "ISAM-Based Nanoscale Thin-Film Devices," Proc. SPIE Smart Structures and Materials Conf. (San Diego), March 1997.

[4] Y. Liu, "Characterization and Patterned Ionic Polymer Films from a Novel Self-Assembly Process," Ph.D. dissertation, Virginia Tech, 1996.

[5] F. Vogtle, *Supramolecular Chemistry*, Wiley, New York, 1993.

[6] J. H. Fuhrhop and J. Koning, *Membrane and Molecular Assemblies, the Synthetic Approach*; Royal Society of Chemistry, London, 1994.

[7] A. Ulman, *An Introduction to Ultrathin Organic Films from Langmuir-Blodgett to Self Assembly*; Academic Press, New York, 1991, Chapter 3.

[8] R. K. Iler, *J. Colloid Interface Science* 1966, 21, 569.

[9] G. Decher and J. Schmitt, *Thin Solid Films* 1992, 210-211.

[10] G. Decher, Y. Lvov, and J. Schmitt, Thin Solid Films **244**, 772 (1994).

[11] Y. Liu, Ph.D. Dissertation, Virginia Tech, 1996.

9.0 Publications and Presentations

The following are recent or current publications or presentations by the research team concerning the ISAM processing of nanoparticle thin-films.

1. Y. Liu, M. B. Miller, K. A. Murphy, R.O. Claus, J. R. Heflin, Y. X. Wang, W. Zhao, "Ionically self-assembled second order nonlinear optical thin-film sensors", Proceedings of SPIE Vol. 3330, March 1998.

2. Y. Liu, M. B. Miller, K. A. Murphy, R. O. Claus, J. R. Heflin, Y. X. Wang, "Functionally tailored nanoparticle-based ionically self-assembled multilayer thin-films", Proceedings of SPIE Vol. 3324, March, 1998.

3. "Molecular Self-Assembly of Ti0$_2$/Polymer Nanocomposite Films," Y. Liu, A. Wang and R.O. Claus, *J. Phys. Chem. B* 1997, 101, p. 1385-1388, February 1997.

4. "Ionic Self-Assembled Monolayer Multi-Layer Thin-Films," Y. Liu, A. Wang and R.O. Claus, Proceedings SPIE Smart Structures & Materials Conference, San Diego

5. "Layer-by-Layer Electrostatic Assembly of Nanoscale Fe$_3$O$_4$ Particles and Polyimide on Silicon and Silica Surfaces," Y. Liu, A. Wang and R. Claus, Proc. MRS Meeting, San Francisco, March 1997.

6. "Blue Light Emitting Nanosized TiO2 Colloids," Y. Liu and R. O. Claus, *J. Am Chem. Soc.*, vol. 30, no. 22, May 1997.

7. "Metallic and Ceramic Nanocomposites with Ionic Self-Assembled Nanoparticle Coatings," R. Claus, Y. Liu and K. Murphy, Proc. 4th Intl. Conf. on Composites Engineering (Kona, Hawaii), July 1997.

8. "Second Order Nonlinear Optical Thin Films Fabricated from Ionically Self-Assembled Monolayers," J. R. Heflin, Y. Liu, C. Figura, D. Marciu and R. Claus, SPIE Annual Meeting (San Diego), August 1997.

9. "Self-Assembled Nanoparticle-Based Multi-Layer Thin-Films and Devices," Y. Liu, J. R. Heflin, W. Zhou and R. Claus, Proc. ARO Smart Materials Workshop, Blacksburg, August 1997.

10. "Noncentrosymmetric Ionically Self-Assembled Thin Films for Second Order Nonlinear Optics," J. R. Heflin, Y. Liu and R.O. Claus, submitted to OSA Thin-Films Conference, Long Beach, CA, September 1997.

11. "Layer-by-layer electrostatic self-assembly of nanoscale Fe_3O_4 particles and polyimide precursor on silicon and silica surfaces," Y. Liu, A. Wang and R.O. Claus, *Appl. Phys. Lett. 71* (16), 20 October 1997.

10. "Self-Assembled Nanoparticle-Based Thin-Film Materials and Devices," R. Claus, seminar to be organized by Dr. Janet Sater, Institute for Defense Analyses (Alexandria, VA), 21 November 1997.

11. "Nanoparticle/Polymer Materials and Devices," Y. Liu and R. Claus, SPIE Smart Structures and Materials Conf., March 1998.

12. "Novel Polymer Dyes for Nonlinear Optical Applications Using ISAM Technology," K.M. Lenahan, Y-X. Wang, Y. Liu, R.O. Claus, J.R. Heflin, D. Marciu and C. Figura, submitted to *Adv. Mater.*

6. Conclusions

During the performance of this STTR Phase I program, F&S along with our development partners at Virginia Tech, have successfully demonstrated the formation of noncentro-symmetric thin films using the ISAM process. These films exhibit significant second-order nonlinear optical properties. Further, we have demonstrated a fabrication process capable of creating thousands of bilayers of such films, which demonstrates the feasibility of full scale commercial manufacturing. The resulting films exhibit significant robustness, particularly during temperature cycling, and do not have to be poled to achieve their nonlinear properties. Finally, we have shown increased performance of the

ISAM films through the synthesis of a number of new polydye materials. These Phase I program results lay the foundation for an expanded product development program based on this technology.